Title

Targeted Genomic Profiling of Acral Melanoma

Journal

Journal of the National Cancer Institute, 111(10)

ISSN

0027-8874

Authors

Yeh, Iwei
Jorgenson, Eric
Shen, Ling
et al.

Publication Date

2019-10-01

DOI

10.1093/jnci/djz005

Peer reviewed

OXFORD

JNCI J Natl Cancer Inst (2019) 111(10): djz005

doi: 10.1093/jnci/djz005
First published online January 18, 2019
Article

ARTICLE

Targeted Genomic Profiling of Acral Melanoma

Iwei Yeh, Eric Jorgenson, Ling Shen, Mengshu Xu, Jeffrey P. North, A. Hunter Shain, David Reuss, Hong Wu, William A. Robinson, Adam Olshen, Andreas von Deimling, Pui-Yan Kwok, Boris C. Bastian*, Maryam M. Asgari*

See the Notes section for the full list of authors' affiliations.
*Authors contributed equally to this work.
Correspondence to: Iwei Yeh, MD, PhD, Departments of Dermatology and Pathology, 1701 Divisadero St. Ste. 280, San Francisco, CA 94115 (e-mail: iwei.yeh@ucsf.edu).

Abstract

Background: Acral melanoma is a rare type of melanoma that affects world populations irrespective of skin color and has worse survival than other cutaneous melanomas. It has relatively few single nucleotide mutations without the UV signature of cutaneous melanomas, but instead has a genetic landscape characterized by structural rearrangements and amplifications. *BRAF* mutations are less common than in other cutaneous melanomas, and knowledge about alternative therapeutic targets is incomplete.
Methods: To identify alternative therapeutic targets, we performed targeted deep-sequencing on 122 acral melanomas. We confirmed the loss of the tumor suppressors p16 and NF1 by immunohistochemistry in select cases.
Results: In addition to *BRAF* (21.3%), *NRAS* (27.9%), and *KIT* (11.5%) mutations, we identified a broad array of MAPK pathway activating alterations, including fusions of *BRAF* (2.5%), *NTRK3* (2.5%), *ALK* (0.8%), and *PRKCA* (0.8%), which can be targeted by available inhibitors. Inactivation of *NF1* occurred in 18 cases (14.8%). Inactivation of the NF1 cooperating factor *SPRED1* occurred in eight cases (6.6%) as an alternative mechanism of disrupting the negative regulation of RAS. Amplifications recurrently affected narrow loci containing *PAK1* and *GAB2* (n = 27, 22.1%), *CDK4* (n = 27, 22.1%), *CCND1* (n = 24, 19.7%), *EP300* (n = 20, 16.4%), *YAP1* (n = 15, 12.3%), *MDM2* (n = 13, 10.7%), and *TERT* (n = 13, 10.7%) providing additional and possibly complementary therapeutic targets. Acral melanomas with $BRAF^{V600E}$ mutations harbored fewer genomic amplifications and were more common in patients with European ancestry.
Conclusion: Our findings support a new, molecularly based subclassification of acral melanoma with potential therapeutic implications: $BRAF^{V600E}$ mutant acral melanomas with characteristics similar to nonacral melanomas that could benefit from BRAF inhibitor therapy, and non-$BRAF^{V600E}$ mutant acral melanomas. Acral melanomas without $BRAF^{V600E}$ mutations harbor a broad array of therapeutically relevant alterations. Expanded molecular profiling would increase the detection of potentially targetable alterations for this subtype of acral melanoma.

ARTICLE

Acral melanomas originate from non-hair-bearing skin of the palms, soles, or nail apparatus. Although it has similar absolute incidence rates across racial-ethnic groups worldwide, it is the most common melanoma subtype in African and Asian populations (1,2). Acral melanoma has poor survival (3) and accounts for a considerable share of melanoma-associated morbidity and mortality worldwide. Whereas melanomas on non-acral skin have a high number of UV-induced mutations (4), acral melanomas have few point mutations, instead harboring increased numbers of structural rearrangements and amplifications (5–7).

It is well established that acral melanomas are driven by mutations in *BRAF*, *NRAS*, *KIT*, and amplifications of *CCND1*, *CDK4*, *MITF*, and *TERT* (8). Individual studies have nominated kinase fusions as drivers in acral melanoma (9,10). Although *BRAF* mutations are common in cutaneous melanoma and an important therapeutic target (11), their frequency in acral melanoma

Received: May 29, 2018; **Revised:** December 12, 2018; **Accepted:** January 4, 2019

is considerably lower (~20% vs ~50%). *BRAF*^{V600E} mutations are common in melanocytic nevi, benign neoplasms that are a risk factor and precursor for melanomas. By contrast, acral melanomas mostly arise from melanoma in situ instead of nevi. Acral melanoma in situ can be subtle with occult disease extending into apparently normal skin, characterized by normal-appearing melanocytes that share pathogenic alterations with adjacent melanoma (8). Thus, the progression of acral melanomas has distinct clinical and genetic features. To provide further insight into the mechanisms of acral melanoma development, we catalogued alterations of genes frequently altered in 122 acral melanomas to further characterize the genetic features of acral melanoma and identify additional therapeutic targets.

Methods

Cases

We searched the archives of Kaiser Permanente Northern California, University of California, San Francisco, Fox Chase Cancer Center, and University of Colorado, Denver for melanoma occurring on the hands and feet. By review of the pathology report and case material, we confirmed the primary melanoma arose on glabrous skin of the palms, soles, or nail unit. We selected the earliest stage of acral melanoma available for each patient (primary, local recurrence, nodal metastasis, distant metastasis). We reviewed a total of 194 cases and excluded those with limiting tumor material (n = 69). We obtained formalin-fixed, paraffin-embedded tissues or DNA extracted from fresh frozen tissue from Kaiser Permanente Northern California (n = 70), University of California, San Francisco (n = 37), Fox Chase Cancer Center (n = 12), and University of Colorado, Denver (n = 6). The study was approved by the Committees on Human Research at each institution and conducted according to the Declaration of Helsinki. Informed consent or a waiver of consent was obtained for each patient. Study data were anonymized to protect subjects' identities.

Sequencing

DNA extracted from tumor tissue was used for sequencing library preparation. Bait libraries targeted the coding regions and select introns of 293 (version 1), 365 (version 2), or 511 (version 3) genes. Sequencing was performed as paired-end 100-bp reads on a HiSeq2000 or 2500 (Illumina, San Diego, CA).

Data were analyzed using Burrows-Wheeler aligner (12), Picard (13), the Genome Analysis Toolkit (14), FreeBayes (15), Delly (16), Annovar (17), THetA2 (18), and CNVkit (19). We excluded samples with mean target coverage below 50× (n = 3, Supplementary Figure 1, available online).

We reviewed truncating mutations and mutations annotated as pathogenic in ClinVar. For genes in which a pathogenic alteration was identified, we annotated all variants of that gene.

Estimation of ancestry composition was performed using 1000 Genomes data (http://www.internationalgenome.org/) (20) and projection analysis by ADMIXTURE (21).

A subset of tumors that lacked RAS/RAF/KIT activating mutations was profiled by targeted RNA-Seq to identify oncogenic fusions (n = 5). Hybrid selection was performed using SureSelect Human Kinome or All ExonV4 kits (Agilent, Santa Clara, CA, p/n 5190–4801, 5190–4631). Sequencing was performed as paired-end 100-bp reads on a HiSeq2500 instrument (Illumina). Fusion detection was performed with Tophat Fusion (22).

Immunohistochemistry

Tissue microarrays were created using cases that had additional tumor material with 2.5-mm cores. NF1 immunohistochemistry was performed using the monoclonal antibody NFC as previously described (23). p16 immunohistochemistry was performed using the CINtec p16 Histology assay (Ventana, Oro Valley, AZ, p/n 725–4713) with dilution of the working antibody 1:10.

Statistical Analysis

Continuous variables were evaluated between conditions using Wilcoxon rank sum tests. Pairs of binary variables were compared using Fisher's exact test. Tests for mutual exclusivity between types of events were performed using elementary probability and under the condition of independence. A multivariable Cox regression model was used to estimate unadjusted hazard ratios and 95% confidence intervals for melanoma-specific mortality. Tests with *P* values less than .05 were considered statistically significant. All statistical tests were two-sided.

Results

BRAF, *RAS*, and *KIT* Mutations

In total 122 acral melanomas (115 primary, seven metastatic, 44.3% male, 55.7% female) were sequenced with a median average target coverage of 289 (Supplementary Table 1, available online). Activating mutations in *BRAF* (n = 26, 21.3%), *RAS* isoforms (n = 39, 32.0%), and *KIT* (n = 14, 11.5%) occurred in a mutually exclusive pattern ($P < .001$; Figure 1). Most *BRAF* mutations resulted in V600E substitution (n = 21, 80.8%) with infrequent V600K (n = 3), K601E (n = 1), and G469S (n = 1) substitutions. *NRAS* was the most frequently mutated RAS isoform (n = 34, 27.9%) with most *NRAS* mutations affecting codon Q61 (n = 26) and the remainder affecting codons G12 or G13 (n = 8). Activating mutations in *HRAS* or *KRAS* occurred in less than 5% of cases.

The mutant *RAS* allele was amplified in four of the 34 (11.8%) tumors with mutant *NRAS*, all three tumors with mutant *KRAS*, and one of two (50.0%) tumors with mutant *HRAS*. Wild-type *KRAS* was amplified in six cases (4.9%), four of which had no mutation in other *RAS* isoforms, *BRAF*, or *KIT*. Activating *KIT* mutations were equally distributed between the juxtamembranous and kinase domains of KIT and amplified in 35.7% of *KIT* mutant cases (Figure 2).

Kinase Fusions

Structural rearrangements resulted in kinase fusions that are known or predicted to activate the MAPK pathway in eight (6.6%) cases. None of these cases had activating mutations in *BRAF*, *RAS* genes, or *KIT*. The *BRAF* fusion genes (n = 3, 2.5%) retained the BRAF kinase domain with loss of the autoinhibitory domain and included *AGK-BRAF* and *ERC1-BRAF*, as previously described (24,25), and a novel *CNTNAP2-BRAF* fusion (Figure 3A; Supplementary Table 2, available online). Similar BRAF fusions occur in Spitz tumors (26).

Fusion genes involving receptor tyrosine kinases occurred in four cases (3.3%), three involving *NTRK3* (2.5%) (Figure 3B) and

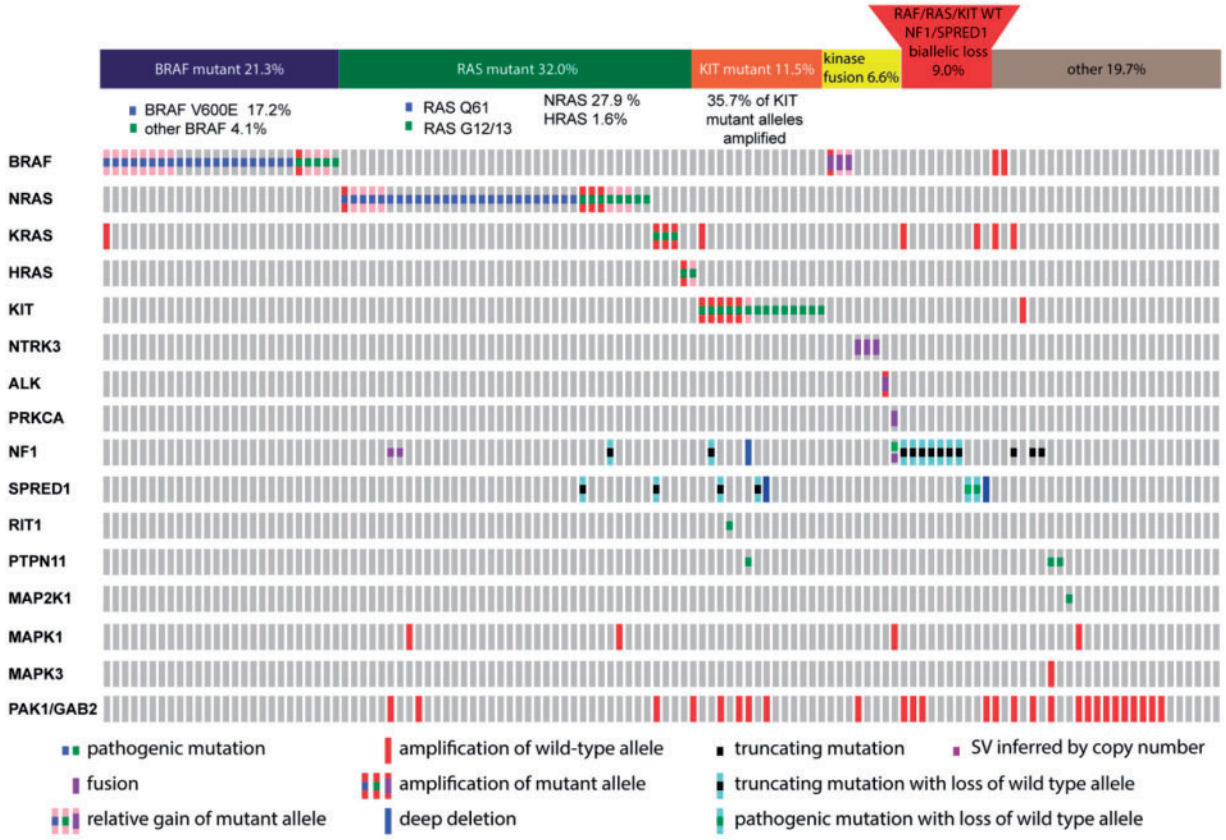

Figure 1. Spectrum of MAPK activating genetic alterations in acral melanoma. Each column represents a single sample (n = 122). Each row indicates reportable findings for each gene(s) as designated by the legend. Many samples have multiple reportable findings.

one involving *ALK* (0.8%). They all contained an intact kinase domain and consisted of *MYO5A-NTRK3* (27), previously described in Spitz tumors, and novel *TUBGCP3-NTRK3* and *SDHA-ALK* fusions. The *SDHA-ALK* fusion gene joined the first intron of *SDHA* to intron 17 of *ALK*, resulting in a predicted out-of-frame transcript and underwent secondary amplification. We suspect the *SDHA-ALK* fusion contains an alternative translation start site that results in a truncated form of the ALK protein with an intact kinase domain.

An *ATP2B4-PRKCA* fusion transcript encoding the kinase domain of protein kinase C alpha was identified by RNA-Seq in a tumor (0.8%) with wild-type *BRAF*, *RAS* genes, and *KIT* (Figure 3C). Similar *ATP2B4-PRKCA* fusions lacking the autoinhibitory domains of *PRKCA* have been reported in pigmented epithelioid melanocytomas (28,29).

RASopathy-Associated Mutations

The RASopathies are genetic syndromes caused by germline mutations in genes involved in MAPK pathway signaling. They include neurofibromatosis and Legius syndrome, which are caused by loss-of-function mutations in *NF1* or *SPRED1*, respectively (30). NF1 promotes RAS deactivation by stimulating its GTPase activity. Losses of *NF1* function resulting from missense mutations, structural rearrangements, or deletions occurred in 16 (13.1%) cases and affected both *NF1* alleles in 10 (8.2%) cases. NF1 expression by immunohistochemistry in evaluable cases was extinguished in all three cases with bi-allelic inactivation, two of four cases with monoallelic truncating mutations, three of 12 (25.0%) cases with single copy deletion of *NF1*, but only two of 65 (3.1%) cases without identifiable genetic alterations of *NF1* (Figure 4A; Supplementary Table 3, available online). These results indicate that in some cases, inactivation of *NF1* occurred by mechanisms not detected by our assay, which could include cryptic rearrangements or epigenetic modifications. Altogether, *NF1* inactivation, evidenced by bi-allelic genetic alterations and/or loss of protein expression, affected 18 (14.8%) cases.

SPRED1 is required for NF1's negative regulation of RAS activity (30) and has recently been identified as a tumor suppressor in mucosal melanoma (31). Loss of function alterations affecting both alleles of *SPRED1* were found in eight (6.6%) cases, none of which harbored *NF1* inactivation. Bi-allelic losses of function of *NF1* or *SPRED1* were mutually exclusive with $BRAF^{V600E}$ mutations ($P = .001$), but concomitant activating alterations in *KIT*, *NRAS*, or *KRAS* were often present (Figure 4B). Notably, either *NF1* or *SPRED1* were lost in six of 14 (42.9%) melanomas with *KIT* mutations ($P = .04$), indicating possible cooperativity between these alterations.

RASopathy-associated mutations in *PTPN11* (n = 3, 2.5%), *MAP2K1* (n = 1, 0.8%), or *RIT1* (n = 1 of 84, 1.2%) were identified in 4% of acral melanomas. The three *PTPN11* mutations (R265Q, Y279C, and A461T) cause Noonan syndrome. Activating mutations in *RIT1* and *MAP2K1* also cause Noonan syndrome (30).

Recurrent Amplifications and Deep Deletions

Many acral melanomas had highly rearranged genomes with amplifications and deep deletions, as previously described

ARTICLE

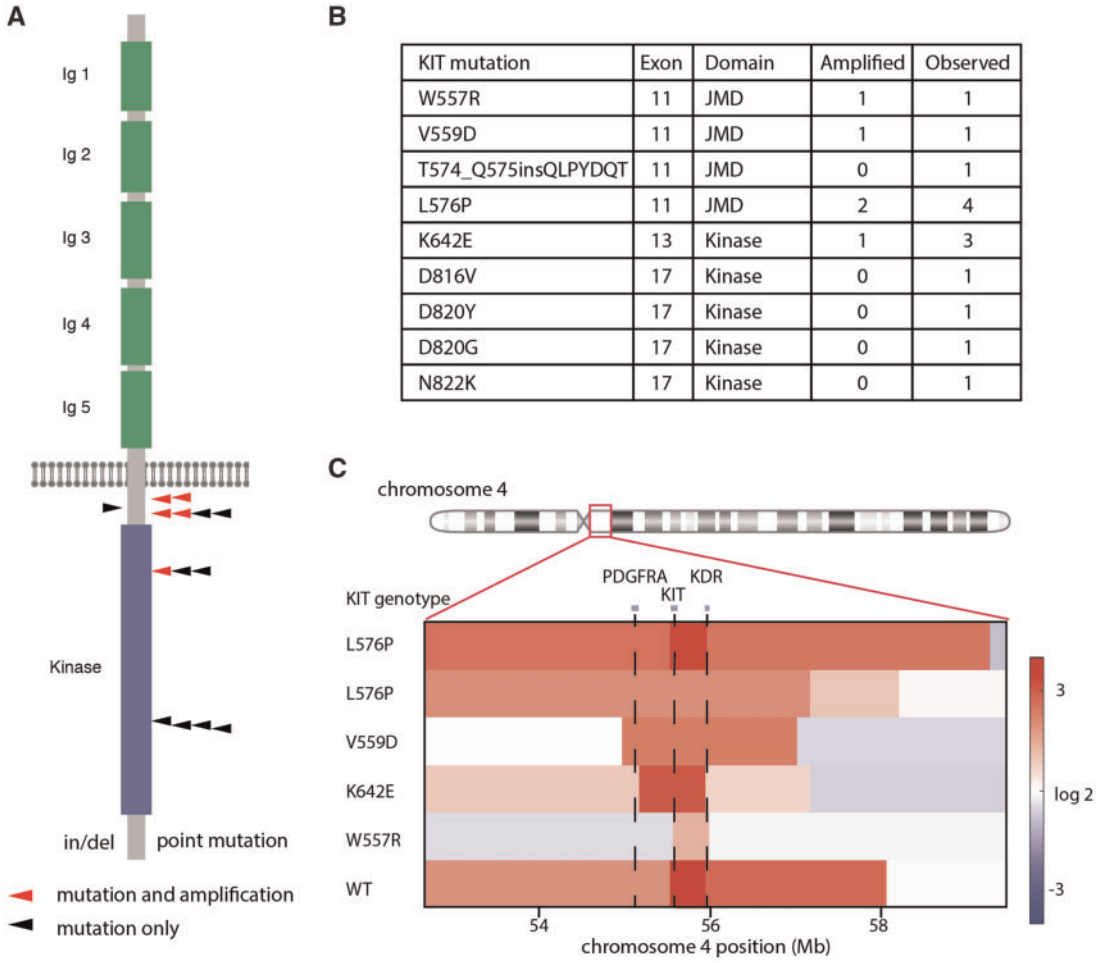

KIT mutation	Exon	Domain	Amplified	Observed
W557R	11	JMD	1	1
V559D	11	JMD	1	1
T574_Q575insQLPYDQT	11	JMD	0	1
L576P	11	JMD	2	4
K642E	13	Kinase	1	3
D816V	17	Kinase	0	1
D820Y	17	Kinase	0	1
D820G	17	Kinase	0	1
N822K	17	Kinase	0	1

Figure 2. *KIT* mutations in acral melanoma. **A)** *KIT* mutations are distributed between the juxtamembranous (JMD) and kinase domains. **B)** Activating mutations occur in various exons of *KIT* and in some cases, the mutant *KIT* allele is amplified. **C)** *KIT* amplification often affects flanking genes *PDGFRA* and *KDR*. Details of the chromosome 4q12 amplicon showing $\log_2$ scaled copy number ratios in *KIT* amplified cases.

(Supplementary Figure 2, available online) (5).The long arm of chromosome 11 harbored three distinct amplicons, located at 11q14 containing *PAK1* and *GAB2* (n = 27, 22.1%); at 11q13 containing *CCND1*, encoding cyclin D1 (n = 24, 19.7%); and at 11q21 containing *YAP1* (n = 15, 12.3%) (Supplementary Figure 3, available online). The regions were co-amplified in many tumors but amplified in isolation in some cases. *PAK1* and *GAB2* are within 1 megabase of each other and were always co-amplified. PAK1 mediates MAPK and Hippo pathway signaling (32,33), whereas GAB2 overexpression increases PI3K signaling and potentiates melanoma invasion (34). *YAP1* is an effector of the Hippo pathway, which regulates contact inhibition of cells, and its amplification and overexpression leads to dysregulated cell growth (35).

Amplifications on chromosome 12 affected *CDK4* at 12q13 in 27 (22.1%) cases and *MDM2* at 12q15 in 13 (10.7%) cases. MDM2 was co-amplified with *CDK4* in more than one-third of *CDK4* amplified cases; however, amplification of *MDM2* without amplification of *CDK4* occurred in four (3.3%) cases.

EP300, on chromosome 22, was amplified in 20 (16.4%) cases. It encodes p300, a transcriptional coactivator with lysine acetyltransferase and E4 ubiquitin ligase activities (36). p300 is a cofactor for MITF (37) and also upregulates p53 transcriptional activity or leads to increased degradation of p53, depending on its cellular context (38,39).

Bi-allelic inactivation of *CDKN2A* occurred in 15 (12.3%) cases, in 14 cases by homozygous deletion. Because *CDKN2A* can be silenced by epigenetic mechanisms, we evaluated expression of its protein product p16 by immunohistochemistry for 85 cases. p16 was not detectable in 45.9%, including all cases with bi-allelic loss, approximately one-half of cases with shallow deletions, and one-third of cases without detected alterations of *CDKN2A* (Supplementary Table 3, available online). These results suggest that, similar to what we observed for NF1, p16 expression can be disrupted by mechanisms not detected by our assay.

Cyclin Dependent Kinase 4/6 Pathway Disruption

CDK4 and CDK6 drive G1 cell-cycle progression by phosphorylating Rb. Both are activated by D-type cyclins and inhibited by p16, p15, and other CDK inhibitors. p16 loss was identified in 36.1% of all cases, either by bi-allelic disruption of *CDKN2A* or loss of p16 expression by immunohistochemistry (Figure 5). p15 is encoded by *CDKN2B*, which is located near *CDKN2A* at 9p21. Loss-of-function single nucleotide variants of *CDKN2B* were not identified, but deep deletions affecting *CDKN2A* also involved *CKDN2B* in all but one case. *CCND2*, which encodes cyclin D2,

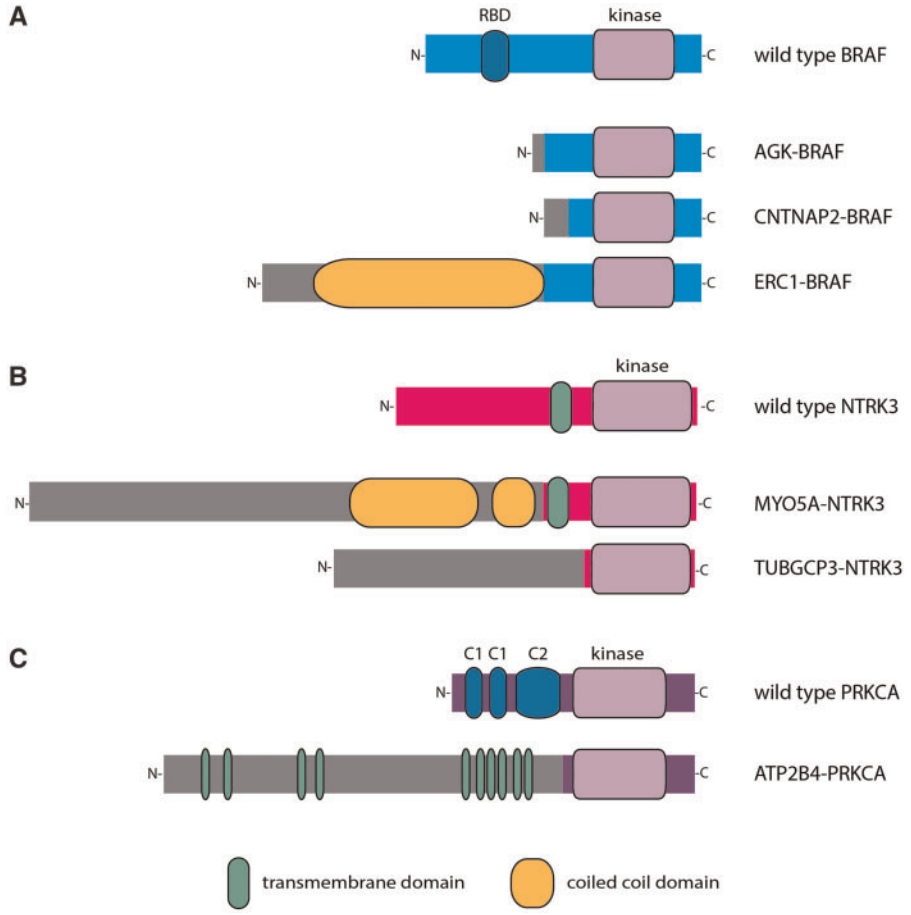

Figure 3. Fusion kinases in acral melanoma. **A**) The *BRAF* fusion junctions reside downstream of the autoinhibitory RAS binding domain (RBD) and upstream of the kinase domain of BRAF. ERC1-BRAF contains a coiled coil domain that promotes dimerization is contributed by ERC1. **B**) The predicted NTRK3 fusion proteins are missing most of the extracellular domain of NTRK3 and may contain the transmembrane domain in addition to the kinase domain. The MYO5A-NTRK3 fusion contains coiled-coil domains contributed by MYO5A. **C**) The predicted ATP2B4-PRKCA fusion protein lacks the regulatory calcium binding domains (C1, C2, C3).

ARTICLE

was amplified in five cases (4.1%) in a mutually exclusive pattern with *CCND1* amplification ($P < .001$). *CDK6* amplification occurred in five cases (4.1%), and in one case *CDK4* amplification was also present. Loss-of-function mutations in *RB1* were not identified. Altogether, activating alterations of the CDK4/6 pathway were identified in 62.3% of cases, with many cases demonstrating alterations in multiple components of the pathway.

p53 Pathway Disruption

The p53 pathway is considered the "guardian of the genome" and triggers cell cycle arrest or apoptosis in response to DNA damage. Although *TP53* is frequently mutated in cancer, melanoma has a comparatively low rate of *TP53* mutation. The high number of structural rearrangements and copy number changes in acral melanoma suggests corruption of the guardian function of the p53 pathway. Nevertheless, *TP53* point mutations were rare in our cohort with only a single pathogenic mutation (H179Q, 0.8%). p53 is antagonized by MDM2, which not only ubiquitinates p53—thereby targeting it for destruction—but also directly binds p53 to inhibit its transcriptional activity (40). MDM4 is homologous to MDM2 and can also bind to p53 and negatively regulate its transcriptional function (41). *MDM4* was amplified in one case (0.8%) in addition to the 13 cases with *MDM2* amplification. The ability of the p53 pathway to respond to DNA damage can also be disrupted by loss of ATM, which phosphorylates p53 in response to double-stranded DNA breaks. Bi-allelic inactivation of *ATM* occurred in six (4.9%) cases, and an additional case demonstrated a single truncating *ATM* mutation. p14ARF, another gene product of *CDKN2A*, inhibits MDM2, and thus loss of *CDKN2A* may contribute to p53 pathway dysfunction. p300 has various effects on p53 activity and increased cytoplasmic p300 leads to decreased p53 levels (38). Altogether, genetic disruption of the p53 pathway was identified in 39.3% of acral melanomas (Figure 6).

TERT Alterations

The majority of melanomas on sun-exposed skin harbor *TERT* promoter mutations (8). *TERT* promoter mutations were uncommon in acral melanoma ($n = 4$ or 5.3% of 75 cases for which *TERT* promoter could be genotyped). Instead, the *TERT* locus was amplified in 13 (10.7%) cases. Almost one-half of the *TERT* amplifications involved a copy number transition within 40 kilobases upstream of *TERT*, indicating that they may alter promoter or enhancer sequences to increase *TERT* expression (42,43). An additional four (3.3%) cases harbored copy number transitions within 40 kb upstream of *TERT* with relative gain of *TERT*, indicating they too may contain altered promoter or enhancer sequences.

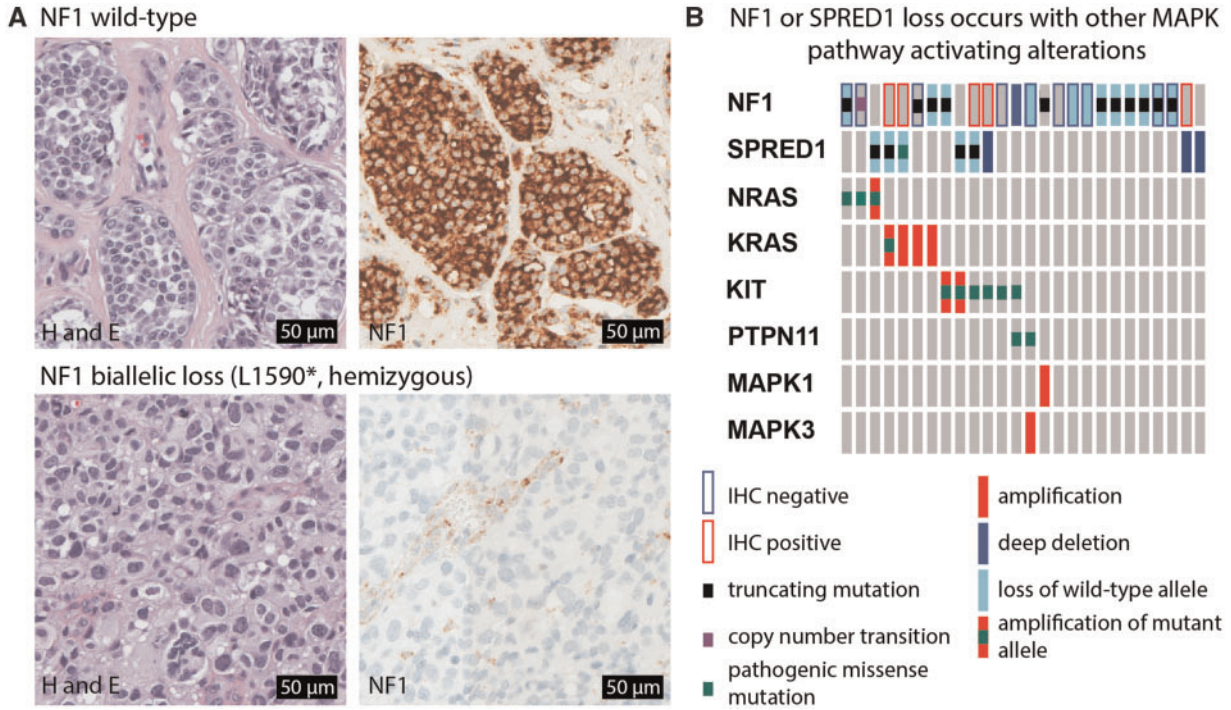

Figure 4. *NF1* and *SPRED1* loss in acral melanoma. **A)** NF1 immunohistochemistry in an acral melanoma without *NF1* mutation (top) shows robust expression of NF1 within neoplastic melanocytes, whereas as expression is lost in a melanoma with a truncating mutation in *NF1* and loss of the wild-type allele (bottom, residual staining is in endothelial cells). **B)** NF1 and SPRED1 loss are mutually exclusive. All cases with bi-allelic loss of *NF1* or *SPRED1* (deep deletion or loss of function mutation with loss of the wild-type allele) and/or absence of NF1 protein expression by immunohistochemistry are shown, one sample per column. Additional MAPK pathway activating alterations are present in a majority of cases.

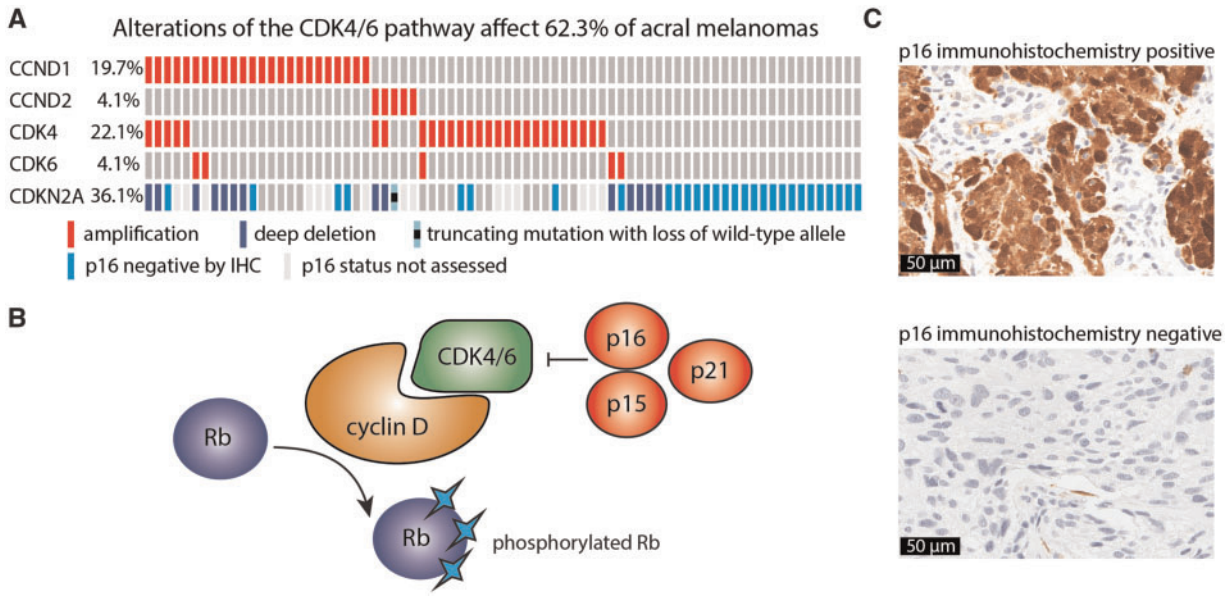

Figure 5. Alterations affecting the CDK4/6 pathway in acral melanoma. **A)** In this tiling plot, each column represents a single sample. Each row indicates reportable findings for each gene(s) as designated by the legend. Many samples have multiple reportable findings. **B)** A pathway diagram shows the interactions of the components of the CDK4/6 pathway. **C)** p16 immunohistochemistry demonstrates loss of expression in cases without bi-allelic inactivation. Acral melanomas with shallow deletion of *CDKN2A* (corresponding to heterozygous loss) demonstrate variable p16 levels by immunohistochemistry. In a case (KAM130) with shallow deletion of *CDKN2A*, strong cytoplasmic and nuclear p16 is present in neoplastic melanocytes (top panel). In another case (KAM34) with shallow deletion of *CDKN2A*, neoplastic melanocytes are negative for p16 by immunohistochemistry (bottom panel). Nuclear p16 positivity is present within endothelial cells.

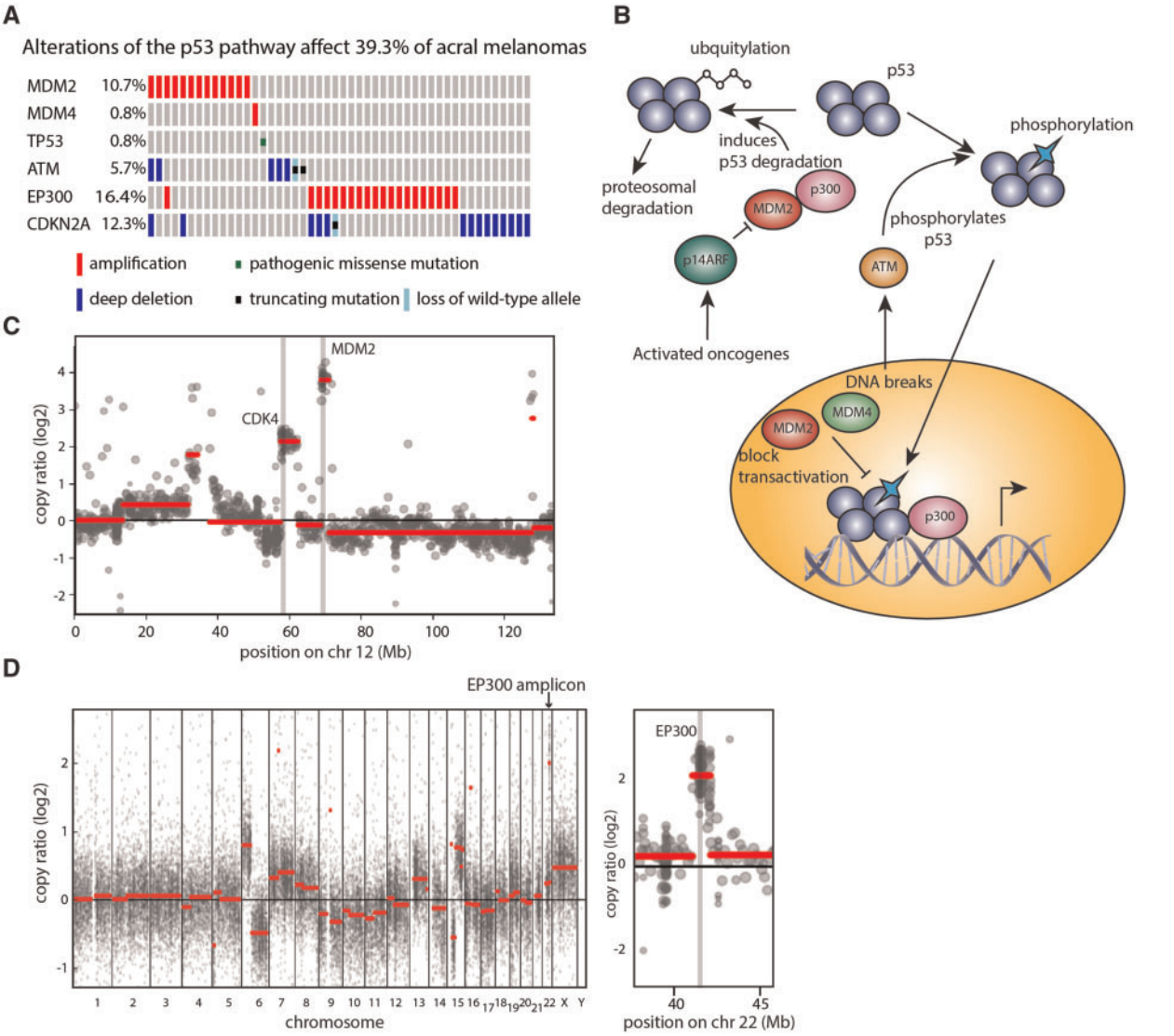

Figure 6. Alterations affecting the p53 pathway in acral melanoma. **A)** In this tiling plot, each column represents a single sample. Each row indicates reportable findings for each gene(s) as designated by the legend. Many samples have multiple reportable findings. **B)** A pathway diagram shows the interactions of the components of the p53 pathway. **C)** Copy number profile of chromosome 12 shows high level amplification of *MDM2* at a higher level than *CDK4* (case MB_1424). **D)** Left: Whole genome copy number profile shows multiple copy number gains and losses and high level amplification of *EP300* (KAM5). Right: Higher resolution view of *EP300* amplification on chromosome 22.

Pathways Recurrently Mutated in Melanoma

Previous genomic studies of melanoma identified mutations affecting various biological pathways (6,44). Although only some members of these pathways were genotyped (Supplementary Table 4, available online), alterations were identified in the histone modification (n = 55, 44.3%), receptor tyrosine kinase (n = 33, 27.0%), WNT signaling (n = 26, 21.3%), PI3K (n = 19, 15.6%), SWI/SNF chromatin remodeling (n = 9, 7.4%), and DNA methylation pathways (n = 4, 3.3%) (Supplementary Figure 4, available online).

Associations Between Clinical and Genetic Features

Melanoma-specific mortality among patients with acral melanoma is associated with tumor thickness and stage at presentation, but not with race or ethnicity (45). Here, in a multivariable Cox survival model predicting melanoma-specific mortality for patients with long-term follow-up information (n = 67) based on *BRAF*, *NRAS*, *KIT*, *CDKN2A*, *CCND1*, *CDK4*, and *EP300* mutation status; age at diagnosis; and sex, only *CDKN2A* bi-allelic inactivation was statistically significantly associated with mortality (hazard ratio = 4.46, 95% confidence interval = 1.11 to 17.87, $P = .03$).

Subungual melanomas may have a particularly poor prognosis (46,47). *KIT* mutation was identified in three of six subungual melanomas, at a greater frequency than in nonsubungual acral melanomas ($P = .03$), whereas *BRAF* or *NRAS* mutations were not associated with subungual location.

Two Subtypes of Acral Melanoma

The $BRAF^{V600E}$ mutations seen in a subset of acral melanomas are typical of melanomas on sun-exposed but not chronically

ARTICLE

Table 1. Potentially actionable alterations in acral melanomas without $BRAF^{V600E}$ mutation

Pathway alterations	Frequency	Targeted therapies	Status of inhibitors
MAPK pathway alterations			
NF1 or SPRED1 bi-allelic loss without RAS, RAF, or KIT mutation	15.8%	MEK inhibitors	Approved for other cancer indications
KIT mutation without bi-allelic loss of NF1 or SPRED1	7.9%	KIT inhibitors	Approved for other cancer indications
KIT mutation with bi-allelic loss of NF1 or SPRED1	5.9%	KIT and/or MEK inhibitors	Approved for other cancer indications
Non-V600E BRAF mutation	5.0%	BRAF and MEK inhibitors	In clinical use, durable responses in a minority of patients
Receptor tyrosine kinase fusion	4.0%	RTK inhibitors (ALK, NTRK inhibitors)	Approved for other cancer indications
BRAF fusion	3.0%	Type IIa BRAF inhibitors and/or MEK inhibitors	Approved for other cancer indications
Protein kinase C fusion	1.0%	PKC inhibitors	Investigational
Other alterations			
CDK4/6 or CCND1/CCND2 amplification, p16 loss	67.3%	CDK4/6 inhibitors	Approved for other cancer indications
PAK1 or YAP1 amplification	29.7%	Verteporfin	Approved for other indications
MDM2 amplification	12.9%	MDM2 inhibitors	Investigational
ATM loss of function	6.9%	PARP inhibitors	Approved for other indications

sun-damaged skin (low-CSD melanomas) typically affecting younger individuals of light complexion (8,48). These melanomas often arise from nevi that harbor $BRAF^{V600E}$. An adjacent nevus was identified in one of the 21 acral melanomas with $BRAF^{V600E}$ mutation. We tested whether $BRAF^{V600E}$ mutations are associated with age, sex, European ancestry, and number of genomic amplifications. $BRAF^{V600E}$ mutations were associated with female sex ($P < .001$) and fewer copy number amplifications (mean 1.9 vs 6.8 amplifications per tumor, $P < .001$). Although patients with $BRAF^{V600E}$ mutations had higher levels of European ancestry, this did not reach statistical significance ($P = .09$). Across mutational studies of acral melanoma in Asian and African populations, $BRAF^{V600E}$ mutations occur in 13.0% compared to 17.2% in our cohort, but this difference was not statistically significant ($P = .34$) (9,49–51). There was no statistically significant difference in age at diagnosis between acral melanomas with or without $BRAF^{V600E}$ mutation. *NRAS* and *KIT* mutations did not show these associations.

Discussion

Our findings suggest the existence of two types of melanoma originating from acral skin. $BRAF^{V600E}$ mutant acral melanomas are similar to melanomas occurring in nonchronically sun-damaged skin (low-CSD melanomas) in that they have fewer DNA copy number changes, may arise from precursor nevi, and European ancestry appears to be a risk factor. Acral melanomas without $BRAF^{V600E}$ mutation comprised 82.8% of cases and are characterized by a broad array of other MAPK activating mutations, a high number of amplifications and rearrangements, and lack of a specific racial predilection. There are several indications that these acral melanomas correspond to what Coleman et al. (52) described as acral lentiginous melanoma. Their characteristic lentiginous growth pattern refers to an in situ component in which increased numbers of single melanocytes are aligned along the basilar epidermis, as opposed to the pagetoid growth pattern of superficial spreading melanoma. Melanomas that arise on chronically sun-damaged skin (high-CSD) also frequently display a lentiginous growth pattern, lack $BRAF^{V600E}$ mutations, and have loss-of-function mutations in *NF1* (53) and activating *KIT* mutations (54). However, they differ from acral melanomas by having a very high point mutation burden and fewer copy number aberrations (53). Several of the novel alterations identified in our study can be linked to the lentiginous growth pattern. Syndromes due to pathogenic mutations in *NF1*, *SPRED1*, *PTPN11*, or *RIT1* are associated with lentigines, café-au-lait macules (30), and high-CSD melanomas (53), all of which have a lentiginous growth pattern, suggesting that these alterations cause lentiginous proliferations of melanocytes.

We identified an extended spectrum of MAPK activating alterations in acral melanomas, including several fusion kinases for which drugs are already in the clinic. Trk inhibitors are showing promising results in early clinical studies in solid tumors with *NTRK* fusions (55), and tumors with *BRAF* fusions including melanomas have responded to BRAF or MEK inhibitors (11). In preclinical studies, MEK inhibitors are effective against some RAS/RAF wild-type melanomas with loss of NF1 (56). Thus, loss-of-function mutations in *SPRED1* or other RASopathy associated mutations would be expected to similarly predict response to MEK inhibition. Loss of *NF1* or *SPRED1* in a clinically significant fraction of *KIT* mutant acral melanomas suggests that combining KIT inhibitors with MEK inhibitors may lead to improved outcomes for these tumors.

Forty percent of acral melanomas in our study lacked targetable MAPK pathway alterations. Although most of these cases harbored activating *RAS* mutations, a subset had no identifiable MAPK activating alteration. Therapeutic targets beyond the MAPK pathway are of particular interest for these tumors as well as for use in combination with existing therapies to prevent drug resistance. Based on our genetic findings, CDK4/6 inhibitors, inhibitors of the MDM2-p53 interaction, and Hippo pathway inhibitors may be effective in acral melanomas with defects in the corresponding pathways.

Our study was limited because we sequenced only targeted regions of the genome and therefore could not discover novel pathogenic point mutations or gene rearrangements.

Additionally, we did not sequence normal DNA from the patients and thus were unable to precisely determine if variants were germline or somatic. To compensate for this, we performed careful annotation and analysis to identify pathogenic or likely pathogenic variants and did not include variants of unknown significance in our analysis.

In conclusion, our study indicates the existence of two distinct melanoma subtypes on acral sites. Acral lentiginous melanomas characterized by the absence of $BRAF^{V600E}$ mutations and many amplifications and structural rearrangements represent the majority of acral melanomas and display considerable diversity of oncogenic drivers, many potentially actionable, which should motivate comprehensive tumor profiling for patients in need of systemic treatment to identify therapeutic targets. By contrast, acral melanomas with $BRAF^{V600E}$ mutations are likely similar to low-CSD melanomas and likely can be treated similarly.

Funding

This work was supported by the Melanoma Research Alliance; Dermatology Foundation; the National Cancer Institute at the National Institutes of Health (grant nos. 5P30CA082103, 1R35CA220481); and the National Institute of Arthritis and Musculoskeletal and Skin at the National Institutes of Health (grant no. K24 AR069760).

Notes

Affiliations of authors: University of California, San Francisco, CA (IY, MX, JPN, AHS, AO, PYK, BCB); Kaiser Permanente Division of Research, Oakland, CA (EJ, LS); Neuropathology, University of Heidelberg and German Cancer Research Center (DKFZ), Heidelberg, Germany (DR, AvD); Fox Chase Cancer Center, Philadelphia, PA (HW); University of Colorado, Denver, CO (WAR); Department of Dermatology, Massachusetts General Hospital, and Department of Population Medicine, Harvard Pilgrim Health Care Institute, Harvard Medical School, Boston, MA (MMA).

The funders had no role in the design of the study; the collection, analysis, and interpretation of the data; the writing of the manuscript; and the decision to submit the manuscript for publication. Drs Yeh and Bastian report grant funding to the University of California, San Francisco from Ignyta, Bayer, and Novartis to support a phase 2 clinical trial on kinase fusions in melanoma. Dr North is a consultant for AdviNOW Medical, outside the submitted work. Dr Reuss and Dr von Deimling report having licensed the NF1 antibody to Cell Marque Corporation. All terms are being managed by the University of Heidelberg in accordance with its conflict of interest policies. Dr Bastian is a consultant for Lilly Inc, outside the submitted work. Dr Asgari reports grant funding to Massachusetts General Hospital from Pfizer Inc and Valeant. The other authors have no disclosures.

We thank Monica Sokil, Alexander Gagnon, and Shanshan Liu for excellent technical assistance.

References

1. Desai A, Ugorji R, Khachemoune A. Acral melanoma foot lesions. Part 1: epidemiology, aetiology, and molecular pathology. *Clin Exp Dermatol*. 2017;42(8):845–848.
2. Durbec F, Martin L, Derancourt C, Grange F. Melanoma of the hand and foot: epidemiological, prognostic and genetic features. A systematic review. *Br J Dermatol*. 2012;166(4):727–739.
3. Bello DM, Chou JF, Panageas KS. Prognosis of acral melanoma: a series of 281 patients. *Ann Surg Oncol*. 2013;20(11):3618–3625.
4. Turajlic S, Furney SJ, Lambros MB, et al. Whole genome sequencing of matched primary and metastatic acral melanomas. *Genome Res*. 2012;22(2):196–207.
5. Curtin JA, Fridlyand J, Kageshita T, et al. Distinct sets of genetic alterations in melanoma. *N Engl J Med*. 2005;353(20):2135–2147.
6. Hayward NK, Wilmott JS, Waddell N, et al. Whole-genome landscapes of major melanoma subtypes. *Nature*. 2017;545(7653):175–180.
7. Liang WS, Hendricks W, Kiefer J, et al. Integrated genomic analyses reveal frequent TERT aberrations in acral melanoma. *Genome Res*. 2017;27(4):524–532.
8. Bastian BC. The molecular pathology of melanoma: an integrated taxonomy of melanocytic neoplasia. *Annu Rev Pathol Mech Dis*. 2014;9(1):239–271.
9. Niu H-T, Zhou Q-M, Wang F, et al. Identification of anaplastic lymphoma kinase break points and oncogenic mutation profiles in acral/mucosal melanomas. *Pigment Cell Melanoma Res*. 2013;26(5):646–653.
10. Turner J, Couts K, Sheren J, et al. Kinase gene fusions in defined subsets of melanoma. *Pigment Cell Melanoma Res*. 2017;30(1):53–62.
11. Luke JJ, Flaherty KT, Ribas A, Long GV. Targeted agents and immunotherapies: optimizing outcomes in melanoma. *Nat Rev Clin Oncol*. 2017;14(8):463–482.
12. Li H, Durbin R. Fast and accurate short read alignment with Burrows-Wheeler transform. *Bioinforma Oxf Engl*. 2009;25(14):1754–1760.
13. Broad Institute. *Picard*. http://broadinstitute.github.io/picard/. version 1.84.
14. McKenna A, Hanna M, Banks E, et al. The Genome Analysis Toolkit: a MapReduce framework for analyzing next-generation DNA sequencing data. *Genome Res*. 2010;20(9):1297–1303.
15. Garrison EMG. Haplotype-based variant detection from short-read sequencing. *arXiv*. 2012;1207.3907. [q-bio.GN].
16. Rausch T, Zichner T, Schlattl A, Stutz AM, Benes V, Korbel JO. DELLY: structural variant discovery by integrated paired-end and split-read analysis. *Bioinformatics*. 2012;28(18):i333–i339.
17. Wang K, Li M, Hakonarson H. ANNOVAR: functional annotation of genetic variants from high-throughput sequencing data. *Nucleic Acids Res*. 2010;38(16):e164.
18. Oesper L, Satas G, Raphael BJ. Quantifying tumor heterogeneity in whole-genome and whole-exome sequencing data. *Bioinformatics*. 2014;30(24):3532–3540.
19. Talevich E, Shain AH, Botton T, Bastian BC. CNVkit: genome-wide copy number detection and visualization from targeted DNA sequencing. *PLOS Comput Biol*. 2016;12(4):e1004873.
20. The 1000 Genomes Project Consortium. A global reference for human genetic variation. *Nature*. 2015;526(7571):68–74.
21. Alexander DH, Novembre J, Lange K. Fast model-based estimation of ancestry in unrelated individuals. *Genome Res*. 2009;19(9):1655–1664.
22. Kim D, Salzberg SL. TopHat-fusion: an algorithm for discovery of novel fusion transcripts. *Genome Biol*. 2011;12(8):R72.
23. Reuss DE, Habel A, Hagenlocher C, et al. Neurofibromin specific antibody differentiates malignant peripheral nerve sheath tumors (MPNST) from other spindle cell neoplasms. *Acta Neuropathol*. 2014;127(4):565–572.
24. Botton T, Yeh I, Nelson T, et al. Recurrent BRAF kinase fusions in melanocytic tumors offer an opportunity for targeted therapy. *Pigment Cell Melanoma Res*. 2013;26(6):845–851.
25. Hovelson DH, McDaniel AS, Cani AK, et al. Development and validation of a scalable next-generation sequencing system for assessing relevant somatic variants in solid tumors. *Neoplasia N Y N*. 2015;17(4):385–399.
26. Wiesner T, He J, Yelensky R, et al. Kinase fusions are frequent in Spitz tumours and spitzoid melanomas. *Nat Commun*. 2014;5:3116.
27. Yeh I, Tee MK, Botton T, et al. NTRK3 kinase fusions in Spitz tumours. *J Pathol*. 2016;240(3):282–290.
28. Bahrami A, Lee S, Wu G, et al. Pigment-synthesizing melanocytic neoplasm with protein kinase C alpha (PRKCA) fusion. *JAMA Dermatol*. 2016;152(3):318–322.
29. Cohen JN, Joseph NM, North JP, Onodera C, Zembowicz A, LeBoit PE. Genomic analysis of pigmented epithelioid melanocytomas reveals recurrent alterations in PRKAR1A, and PRKCA genes. *Am J Surg Pathol*. 2017;41(10):1333–1346.
30. Tidyman WE, Rauen KA. Pathogenetics of the RASopathies. *Hum Mol Genet*. 2016;25(R2):R123–R132.
31. Ablain J, Xu M, Rothschild H, et al. Human tumor genomics and zebrafish modeling identify SPRED1 loss as a driver of mucosal melanoma. *Science*. 2018;362(6418):1055–1060.
32. Ong CC, Jubb AM, Jakubiak D, et al. P21-activated kinase 1 (PAK1) as a therapeutic target in BRAF wild-type melanoma. *J Natl Cancer Inst*. 2013;105(9):606–607.
33. Sabra H, Brunner M, Mandati V, et al. β1 integrin–dependent Rac/group I PAK signaling mediates YAP activation of Yes-associated protein 1 (YAP1) via NF2/merlin. *J Biol Chem*. 2017;292(47):19179–19197.
34. Horst B, Gruvberger-Saal SK, Hopkins BD, et al. Gab2-mediated signaling promotes melanoma metastasis. *Am J Pathol*. 2009;174(4):1524–1533.

ARTICLE

35. Zhao B, Wei X, Li W, et al. Inactivation of YAP oncoprotein by the Hippo pathway is involved in cell contact inhibition and tissue growth control. *Genes Dev*. 2007;21(21):2747–2761.
36. Wang F, Marshall CB, Ikura M. Transcriptional/epigenetic regulator CBP/p300 in tumorigenesis: structural and functional versatility in target recognition. *Cell Mol Life Sci CMLS*. 2013;70(21):3989–4008.
37. Sato S, Roberts K, Gambino G, Cook A, Kouzarides T, Goding CR. CBP/p300 as a co-factor for the Microphthalmia transcription factor. *Oncogene*. 1997;14(25): 3083–3092.
38. Shi D, Pop MS, Kulikov R, Love IM, Kung AL, Grossman SR. CBP and p300 are cytoplasmic E4 polyubiquitin ligases for p53. *Proc Natl Acad Sci*. 2009;106(38): 16275–16280.
39. Lill NL, Grossman SR, Ginsberg D, DeCaprio J, Livingston DM. Binding and modulation of p53 by p300/CBP coactivators. *Nature*. 1997;387(6635):823–827.
40. Pellegrino M, Mancini F, Lucà R, et al. Targeting the MDM2/MDM4 interaction interface as a promising approach for p53 reactivation therapy. *Cancer Res*. 2015;75(21):4560–4572.
41. Parant J, Chavez-Reyes A, Little NA, et al. Rescue of embryonic lethality in Mdm4-null mice by loss of Trp53 suggests a nonoverlapping pathway with MDM2 to regulate p53. *Nat Genet*. 2001;29(1):92–95.
42. Davis CF, Ricketts CJ, Wang M, et al. The somatic genomic landscape of chromophobe renal cell carcinoma. *Cancer Cell*. 2014;26(3):319–330.
43. Peifer M, Hertwig F, Roels F, et al. Telomerase activation by genomic rearrangements in high-risk neuroblastoma. *Nature*. 2015;526(7575):700–704.
44. Akbani R, Akdemir KC, Aksoy BA, et al. Genomic classification of cutaneous melanoma. *Cell*. 2015;161(7):1681–1696.
45. Asgari MM, Shen L, Sokil MM, Yeh I, Jorgenson E. Prognostic factors and survival in acral lentiginous melanoma. *Br J Dermatol*. 2017;177(2):428–435.
46. Patterson RH, Helwig EB. Subungual malignant melanoma: a clinical—pathologic study. *Cancer*. 1980;46(9):2074–2087.
47. Cohen T, Busam KJ, Patel A, Brady MS. Subungual melanoma: management considerations. *Am J Surg*. 2008;195(2):244–248.
48. Elder DE, Massi D, Scolyer R, Willemze R. *WHO Classification of Skin Tumours*. 4th ed. Lyon, France: IARC Press; 2018.
49. Si L, Kong Y, Xu X, et al. Prevalence of BRAF V600E mutation in Chinese melanoma patients: large scale analysis of BRAF and NRAS mutations in a 432-case cohort. *Eur J Cancer*. 2012;48(1):94–100.
50. Hong J-W, Lee S, Kim D-C, Kim K-H, Song K-H. Prognostic and clinicopathologic associations of BRAF mutation in primary acral lentiginous melanoma in Korean patients: a preliminary study. *Ann Dermatol*. 2014;26(2): 195–202.
51. Puntervoll HE, Molven A, Akslen LA. Frequencies of KIT and GNAQ mutations in acral melanoma. *J Cutan Pathol*. 2014;41(11):893–894.
52. Coleman WP, Loria PR, Reed RJ, Krementz ET. Acral lentiginous melanoma. *Arch Dermatol*. 1980;116(7):773–776.
53. Krauthammer M, Kong Y, Bacchiocchi A, et al. Exome sequencing identifies recurrent mutations in NF1 and RASopathy genes in sun-exposed melanomas. *Nat Genet*. 2015;47(9):996–1002.
54. Curtin JA, Busam K, Pinkel D, Bastian BC. Somatic activation of KIT in distinct subtypes of melanoma. *J Clin Oncol*. 2006;24(26):4340–4346.
55. Drilon A, Laetsch TW, Kummar S, et al. Efficacy of larotrectinib in TRK fusion–positive cancers in adults and children. *N Engl J Med*. 2018;378(8): 731–739.
56. Nissan MH, Pratilas CA, Jones AM, et al. Loss of NF1 in cutaneous melanoma is associated with RAS activation and MEK dependence. *Cancer Res*. 2014; 74(8):2340–2350.